Low-energy electron-He scattering in a low-frequency laser field

N. J. Kylstra[1] and C. J. Joachain[2,3]
[1]*Optics Section, Blackett Laboratory, Imperial College, London SW7 2BZ, United Kingdom*
[2]*Physique Théorique, Faculté des Sciences, Code Postal 227, Université Libre de Bruxelles, B-1050 Brussels, Belgium*
[3]*Max-Planck-Institut für Quantenoptik, D-8046 Garching, Germany*
(Received 5 March 1999)

A method for calculating the laser-assisted, electron-potential scattering differential cross section that is based on the Floquet-Lippmann-Schwinger equation is presented. The method is applied to the laser-assisted, low-energy electron-helium scattering in a CO_2 laser field, in the static no-exchange approximation, for the scattering geometry in which the polarization vector of the laser field is parallel to the direction of the incident electron. We compare our results with the low-frequency approximation of Kroll and Watson [Phys. Rev. A **8**, 804 (1973)] and find, overall, reasonable agreement. An alternative derivation of the Kroll and Watson low-frequency approximation, starting from the Floquet-Lippmann-Schwinger equation, is given in an appendix. [S1050-2947(99)11208-3]

PACS number(s): 34.80.Qb, 03.65.Nk, 32.80.Wr

I. INTRODUCTION

In a variety of scattering processes involving the interaction of electromagnetic radiation and charged particles, a low-frequency limit for the differential scattering cross section can be obtained that factors into the elastic differential cross section times a factor that depends on the electromagnetic field and the momentum transfer of the projectile (for a recent review, see, e.g., [1]). For the scattering of fast electrons by a potential in an intense laser field, this factorization can be readily demonstrated when the projectile-potential interaction is treated in the first Born approximation [2]. Kroll and Watson [3] have shown that such a factorization is possible for the scattering of slow electrons in a low-frequency laser field, with the first Born elastic differential cross section replaced by the exact, field-free differential cross section evaluated with shifted initial and final projectile momenta. The low-frequency requirement is that the incident electron energy be much larger than the photon energy. This elegant low-frequency approximation (LFA) has been subsequently examined theoretically by a number of authors (see, e.g., [1,4,5]). A particular feature of the LFA is that when the projectile momentum transfer becomes perpendicular to the polarization vector of the laser field, the approximations leading to the derivation of the LFA break down. At these, henceforth to be called critical, geometries there is no reason to expect *a priori* that the LFA will give an accurate approximation of the true differential scattering cross section.

Experiments have been carried out by Wallbank *et al.* [6] in which the differential cross sections for the scattering of electrons by argon in the presence of an intense CO_2 laser field have been measured far from the critical geometry, i.e., for momentum transfers nearly parallel to the laser polarization. Good agreement with the LFA was obtained, once the experimental conditions were accounted for (see, e.g., [1]). In more recent experiments performed near the critical geometry, Wallbank and Holmes [7] have measured differential cross sections that differ by many orders of magnitude from those predicted by the LFA. These experimental results have renewed theoretical interest in the Kroll and Watson LFA [8–22], in particular with respect to its validity at the critical geometries. However, these theoretical studies have provided conflicting assessments of the LFA, with reasonable agreement being found by some authors and differences of many orders of magnitude being obtained by others (see, e.g., [21]). We note that it has been pointed out that double scattering could play an important role under the experimental conditions [13,17].

We have recently addressed the issue of the validity of the LFA at the critical geometries by numerically solving the Floquet-Lippmann-Schwinger equation (FLSE) for electron-potential scattering in a CO_2 laser field [21]. In this paper we discuss in detail the theory underlying our method and we continue our investigation of the validity of the LFA by considering laser-assisted, low-energy electron-helium scattering in a CO_2 laser field, in the static no-exchange approximation. The scattering geometry considered is the one in which the polarization vector of the laser field is parallel to the direction of the incident electron. In this geometry, the momentum transfer becomes perpendicular to the laser polarization direction for small-angle scattering. In the following section we formulate the theory of laser-assisted electron-potential scattering and we derive the FLSE that is used as the basis for our numerical calculations. Our formulation of the problem falls within the framework of the usual time-dependent scattering theory [23]; however, we remove the time dependence from the time-dependent Lippmann-Schwinger equation from the onset by writing the scattering wave functions in the Floquet-Fourier form [24]. This formalism is akin to that obtained when quantizing the electromagnetic field [25]. We then introduce the partial-wave form of the FLSE. In the last section we discuss some of the numerical aspects of our approach, and results are presented for the laser-assisted electron-He scattering cross section in the static no-exchange approximation. Finally, we give in the appendixes a brief derivation of the Kroll and Watson result, starting from the FLSE, and discuss in further detail some aspects of our approach. Unless otherwise indicated, atomic units (a.u.) are used throughout.

II. THEORY

A. Basic formalism

The time-dependent Hamiltonian governing the laser-assisted electron-potential scattering dynamics is

$$H(t)=H_0+H_{\rm int}(t)+V. \tag{2.1}$$

Here the free-particle Hamiltonian is H_0, the electron-laser interaction is given by $H_{\rm int}(t)$, with

$$H_{\rm int}(t)=\frac{1}{c}\mathbf{A}(t)\cdot\mathbf{p}+\frac{1}{2c^2}A^2(t), \tag{2.2}$$

and V is the potential from which the electron scatters. The $A^2(t)$ term in the Hamiltonian can be removed by a gauge transformation, and in what follows we assume that this transformation has been performed. The laser field is described classically as a monomode, linearly-polarized, time-dependent electric field and in the dipole approximation. A formal solution of the time-dependent Schrödinger equation,

$$\mathrm{i}\frac{\partial}{\partial t}|\Psi(t)\rangle=H(t)|\Psi(t)\rangle, \tag{2.3}$$

can be cast in the form of the time-dependent Lippmann-Schwinger equation (see, e.g., [23]),

$$|\Psi_a^{(+)}(t)\rangle=|\chi_a(t)\rangle+\int_{-\infty}^{t}dt'K^{(+)}(t,t')V|\Psi_a^{(+)}(t')\rangle, \tag{2.4}$$

where the subscript a refers to the initial state. The states $|\chi_a(t)\rangle$ are solutions of the time-dependent Schrödinger equation in the absence of the potential V,

$$\mathrm{i}\frac{\partial}{\partial t}|\chi(t)\rangle=[H_0+H_{\rm int}(t)]|\chi(t)\rangle, \tag{2.5}$$

and $K^{(+)}(t,t')$ is the associated causal propagator satisfying

$$\left(\mathrm{i}\frac{\partial}{\partial t}-H_0-H_{\rm int}(t)\right)K^{(+)}(t,t')=\delta(t-t'). \tag{2.6}$$

Scattering information is then obtained by calculating the S-matrix elements

$$\begin{aligned}S_{ba}&=\lim_{t\to+\infty}\langle\Psi_b^{(-)}(t)|\Psi_a^{(+)}(t)\rangle\\&=\delta_{b,a}-\mathrm{i}\int_{-\infty}^{\infty}dt\langle\chi_b(t)|V|\Psi_a^{(+)}(t)\rangle,\end{aligned} \tag{2.7}$$

from which the required scattering cross sections can be determined.

For pulse durations that are sufficiently long so that, on average, the laser intensity does not vary much from its peak intensity on times scales that are of the order of typical ''scattering times,'' we can describe the scattering process in terms of time-independent transition rates. In this adiabatic limit, the laser can be taken to be monochromatic. The vector potential can then be written as

$$\mathbf{A}(t)=\mathbf{A}_0\cos\omega t, \tag{2.8}$$

with

$$\mathbf{A}_0=\hat{\boldsymbol{\epsilon}}A_0=\hat{\boldsymbol{\epsilon}}\frac{c\mathcal{E}_0}{\omega}, \tag{2.9}$$

where $\hat{\boldsymbol{\epsilon}}$ is the polarization direction, $\mathcal{E}_0$ is the peak electric-field strength, and ω is the laser angular frequency. Since the Hamiltonian (2.1) is periodic in time, with period $2\pi/\omega$, the states $|\Psi_a^{(+)}(t)\rangle$ and $|\chi_b(t)\rangle$ can be written in the Floquet-Fourier form (see, e.g., [24])

$$|\Psi_a^{(+)}(t)\rangle=\exp(-\mathrm{i}E_at)\sum_{l=-\infty}^{\infty}\exp(-\mathrm{i}l\omega t)|F_{a,l}^{(+)}\rangle, \tag{2.10}$$

$$|\chi_b(t)\rangle=\exp(-\mathrm{i}E_bt)\sum_{l=-\infty}^{\infty}\exp(-\mathrm{i}l\omega t)|f_{b,l}\rangle. \tag{2.11}$$

Inserting these Floquet-Fourier expansions into Eq. (2.7), one obtains for the S-matrix elements

$$\begin{aligned}S_{ba}&=\delta_{b,a}-2\pi\mathrm{i}\sum_{k,l=-\infty}^{\infty}\delta(E_a-E_b-\omega(k-l))\langle f_{b,k}|V|F_{a,l}^{(+)}\rangle\\&=\delta_{b,a}-2\pi\mathrm{i}\sum_{k=-\infty}^{\infty}\delta(E_a-E_b-\omega k)\\&\quad\times\sum_{l=-\infty}^{\infty}\langle f_{b,k+l}|V|F_{a,l}^{(+)}\rangle.\end{aligned} \tag{2.12}$$

The required transition-matrix, or T-matrix, element is

$$T_{ba}^k=\sum_{l=-\infty}^{\infty}\langle f_{b,k+l}|V|F_{a,l}^{(+)}\rangle, \tag{2.13}$$

from which the differential cross section for the scattering of an electron having initial energy E_a, into the solid angle $d\Omega$ centered about the direction (θ,ϕ), is

$$\frac{d\sigma_{ba}^k}{d\Omega}=(2\pi)^4\frac{p_b}{p_a}|T_{ba}^k|^2, \tag{2.14}$$

with $p_a=\sqrt{2E_a}$, $p_b=\sqrt{2(E_a-k\omega)}$. In our notation, k is the number of photons emitted during the collision, so that positive values of k correspond to emission and negative ones to absorption.

We now obtain an integral equation for the T-matrix element T_{ba}^k. Inserting the Floquet-Fourier expansions (2.11) and (2.10) as well as the following representation for the propagator

$$K^{(+)}(t,t')=-\mathrm{i}\theta(t-t')\sum_i|\chi_i(t)\rangle\langle\chi_i(t')|, \tag{2.15}$$

where the sum is over a complete set of solutions of Eq. (2.5), into Eq. (2.4), and carrying out the time integration, the Floquet-Fourier coefficients are found to satisfy the time-independent FLSE

$$|F_{a,l}^{(+)}\rangle = |f_{a,l}\rangle + \sum_i \sum_{m,n=-\infty}^{\infty} |f_{i,l+m}\rangle \times \frac{1}{E_a-(E_i+m\omega)+i\epsilon}\langle f_{i,n+m}|V|F_{a,n}^{(+)}\rangle. \quad (2.16)$$

In order to obtain an expression for the scattering transition amplitudes, we first premultiply this equation by $\langle f_{b,k+l}|V$,

$$\langle f_{b,k+l}|V|F_{a,l}^{(+)}\rangle = \langle f_{b,k+l}|V|f_{a,l}\rangle + \sum_i \sum_{m,n=-\infty}^{\infty} \langle f_{b,k+l}|V|f_{i,l+m}\rangle \times \frac{1}{E_a-(E_i+m\omega)+i\epsilon}\langle f_{i,n+m}|V|F_{a,n}^{(+)}\rangle. \quad (2.17)$$

Now defining the quantities

$$V_{ij}^{k-m} = \sum_{l=-\infty}^{\infty} \langle f_{i,k+l}|V|f_{j,l+m}\rangle, \quad (2.18)$$

and using Eq. (2.13), the on-energy shell T-matrix elements T_{ba}^k are found to satisfy the Floquet-Lippmann-Schwinger equation (FLSE)

$$T_{ba}^k = V_{ba}^k + \sum_i \sum_{m=-\infty}^{\infty} V_{bi}^{k-m} \frac{1}{E_a-(E_i+m\omega)+i\epsilon} T_{ia}^m. \quad (2.19)$$

This is the fundamental equation to be solved. Note that $T_{ba}^k = T_{ab}^{-k}$. We also define the off-the-energy-shell T-matrix elements $T_{ba}^{(+)k}(E)$ by

$$T_{ba}^{(+)k}(E) = V_{ba}^k + \sum_i \sum_{m=-\infty}^{\infty} V_{bi}^{k-m} \times \frac{1}{E-(E_i+m\omega)+i\epsilon} T_{ia}^{(+)m}(E). \quad (2.20)$$

The solution of the time-dependent Schrödinger equation (2.5) is the well-known Gordon-Volkov wave function

$$\chi_{\mathbf{p}}(\mathbf{r},t) = (2\pi)^{-3/2}\exp[i(\mathbf{p}\cdot\mathbf{r} - \mathbf{p}\cdot\boldsymbol{\alpha}(t) - Et)], \quad (2.21)$$

where $E = p^2/2$ and

$$\boldsymbol{\alpha}(t) = \frac{1}{c}\int^t \mathbf{A}(t')dt' = \boldsymbol{\alpha}_0 \sin\omega t \quad (2.22)$$

corresponds to the quiver motion of a free, classical electron in a monochromatic laser field. Setting $\boldsymbol{\alpha}_0 = \hat{\boldsymbol{\epsilon}}\alpha_0$, the quantity

$$\alpha_0 = \frac{\mathcal{E}_0}{\omega^2} \quad (2.23)$$

is the oscillation amplitude of the electron in the laser field. From Eq. (2.21), and using the generating function for the Bessel function, the functions $f_{\mathbf{p},l}(\mathbf{r}) = \langle \mathbf{r}|f_{\mathbf{p},l}\rangle$ appearing in the Floquet-Fourier expansion (2.11), are readily found to be

$$f_{\mathbf{p},l}(\mathbf{r}) = (2\pi)^{-3/2} J_l(\mathbf{p}\cdot\boldsymbol{\alpha}_0)\exp(i\mathbf{p}\cdot\mathbf{r}), \quad (2.24)$$

with J_l being an ordinary Bessel function. The required potential matrix elements, Eq. (2.18), are

$$V_{\mathbf{p}_i,\mathbf{p}_j}^{k-m} = \sum_{l=-\infty}^{\infty} \langle f_{\mathbf{p}_i,k+l}|V|f_{\mathbf{p}_j,m+l}\rangle = \sum_{l=-\infty}^{\infty} J_{k+l}(\mathbf{p}_i\cdot\boldsymbol{\alpha}_0)J_{l+m}(\mathbf{p}_j\cdot\boldsymbol{\alpha}_0)\langle \mathbf{p}_i|V|\mathbf{p}_j\rangle = J_{k-m}(\boldsymbol{\Delta}_{ij}\cdot\boldsymbol{\alpha}_0)\langle \mathbf{p}_i|V|\mathbf{p}_j\rangle, \quad (2.25)$$

with $\boldsymbol{\Delta}_{ij} = \mathbf{p}_i - \mathbf{p}_j$. The FLSE to be solved now takes the form

$$T_{\mathbf{p}_b,\mathbf{p}_a}^{(+)k}(E) = J_k(\boldsymbol{\Delta}_{ba}\cdot\boldsymbol{\alpha}_0)\langle \mathbf{p}_b|V|\mathbf{p}_a\rangle + \sum_{m=-\infty}^{\infty} \int d\mathbf{p}_i J_{k-m}(\boldsymbol{\Delta}_{bi}\cdot\boldsymbol{\alpha}_0) \times \frac{\langle \mathbf{p}_b|V|\mathbf{p}_i\rangle}{E-(E_i+m\omega)+i\epsilon} T_{\mathbf{p}_i,\mathbf{p}_a}^{(+)m}(E). \quad (2.26)$$

This integral equation can be solved using standard numerical methods. The size of the problem is effectively given by the number of Fourier components retained in the Floquet-Fourier expansion times the number of grid points in three dimensions retained in the evaluation of the integral. Since we will be concerned with scattering at low energies, where only a limited number of partial waves contribute to the cross section, the angular integrations can be efficiently carried out by expanding the FLSE in terms of partial waves, as will be discussed in Sec. III B.

B. Partial-wave FLSE

Generally, the T matrix can be expanded as

$$T_{\mathbf{p}_i,\mathbf{p}_j}^{(+)k}(E) = \sum_{L,L'=0}^{\infty} \sum_{K=0}^{\infty} \sum_{Q=-K}^{K} Y_{LL'}^{KQ}(\hat{\mathbf{p}}_i,\hat{\mathbf{p}}_j) T_{p_i,p_j,LL'}^{(+)k,KQ}(p), \quad (2.27)$$

where the $Y_{LL'}^{KQ}$ are coupled spherical harmonics. Choosing our coordinate system such that the laser polarization vector defines the quantization axis,

$$\hat{\boldsymbol{\epsilon}} = \hat{\mathbf{z}}, \quad (2.28)$$

and noting that the Hamiltonian remains invariant under rotations about this axis, the above expression simplifies to

$$T_{\mathbf{p}_i,\mathbf{p}_j}^{(+)k}(E) = \sum_{L,L'=0}^{\infty} \sum_{K=0}^{\infty} Y_{LL'}^{K0}(\hat{\mathbf{p}}_i,\hat{\mathbf{p}}_j) T_{p_i,p_j,LL'}^{(+)k,K0}(p). \quad (2.29)$$

If we now restrict ourselves to the geometry discussed in the Introduction, i.e., the geometry in which the direction of the incident electron coincides with the laser polarization,

$$\hat{\boldsymbol{\epsilon}}=\hat{\mathbf{p}}_a, \tag{2.30}$$

the above partial-wave decomposition of the T-matrix element reduces to

$$T^{(+)k}_{\mathrm{p}_b,\mathrm{p}_a}(E)=\frac{1}{4\pi}\sum_{L=0}^{\infty}[L]P_L(\cos\theta)T^{(+)k}_{p_b,p_a,L}(p). \tag{2.31}$$

The scattering angle, i.e., the angle between the vectors $\mathbf{p}_b$ and $\mathbf{p}_a$, is θ and we use the notation $[L]=2L+1$. Likewise, we expand the potential matrix elements as

$$\langle\mathbf{p}_i|V|\mathbf{p}_j\rangle=\sum_{l=0}^{\infty}\sum_{m=-l}^{l}Y_{lm}(\hat{\mathbf{p}}_i)Y^*_{lm}(\hat{\mathbf{p}}_j)V_l(p_i,p_j), \tag{2.32}$$

and we write

$$\begin{aligned}J_k(\boldsymbol{\Delta}_{ij}\cdot\boldsymbol{\alpha}_0)&=\sum_{l,l'=0}^{\infty}\sum_{m,m'}Y_{lm}(\hat{\mathbf{p}}_i)Y^*_{lm}(\hat{\boldsymbol{\alpha}}_0)Y_{l'm'}(\hat{\mathbf{p}}_j)Y^*_{l'm'}(\hat{\boldsymbol{\alpha}}_0)\mathcal{J}^k_{l,l'}(p_i\alpha_0,p_j\alpha_0)\\&=\frac{1}{(4\pi)^2}\sum_{l,l'=0}^{\infty}[l,l']P_l(\cos\theta_i)P_{l'}(\cos\theta_j)\mathcal{J}^k_{l,l'}(p_i\alpha_0,p_j\alpha_0),\end{aligned} \tag{2.33}$$

where in the second step we have used Eq. (2.30). The functions $\mathcal{J}^k_{l,l'}$ are discussed in Appendix D. With these partial-wave expansions, the resulting partial-wave FLSE is

$$T^{(+)k}_{p_b,p_a,L}(p)=\mathcal{V}^k_L(p_b,p_a,\alpha_0)+2\sum_{m=-\infty}^{\infty}\sum_{L'=0}^{\infty}[L']\int p_i^2dp_i\,\frac{\mathcal{V}^{k-m}_{L,L'}(p_b,p_i,\alpha_0)T^{(+)m}_{p_i,p_a,L'}(p)}{p^2-(p_i^2+2m\omega)+\mathrm{i}\epsilon}. \tag{2.34}$$

The partial-wave potential matrix elements are

$$\mathcal{V}^k_{L,L'}(p_i,p_j,\alpha_0)=\frac{1}{(4\pi)^2}\sum_{l,l',l''=0}^{\infty}[l,l',l'']\begin{pmatrix}l&l''&L\\0&0&0\end{pmatrix}^2\begin{pmatrix}l'&l''&L'\\0&0&0\end{pmatrix}^2\mathcal{J}^k_{l,l'}(p_i\alpha_0,p_j\alpha_0)V_{l''}(p_i,p_j) \tag{2.35}$$

and

$$\begin{aligned}\mathcal{V}^k_L(p_i,p_j,\alpha_0)&=\sum_{L'=0}^{\infty}[L']\mathcal{V}^k_{L,L'}(p_i,p_j,\alpha_0)\\&=\frac{1}{(4\pi)^2}\sum_{l,l',l''=0}^{\infty}[l,l,l'']\begin{pmatrix}l&l''&L\\0&0&0\end{pmatrix}^2\mathcal{J}^k_{l,l'}(p_i\alpha_0,p_j\alpha_0)V_{l''}(p_i,p_j).\end{aligned} \tag{2.36}$$

The required on-shell T-matrix elements satisfy

$$\begin{aligned}T^k_{p_b,p_a,L}(p_a)&=\mathcal{V}^k_L(p_b,p_a,\alpha_0)+2\sum_{m=-\infty}^{\infty}\sum_{L'=0}^{\infty}[L']\\&\times\left(\mathcal{P}\int p_i^2dp_i\,\frac{\mathcal{V}^{k-m}_{L,L'}(p_b,p_i,\alpha_0)T^m_{p_i,p_a,L'}(p_a)}{p_a^2-(p_i^2+2m\omega)}-\mathrm{i}\pi k_b\mathcal{V}^{k-m}_{L,L'}(p_b,p_b,\alpha_0)T^m_{p_b,p_a,L'}(p_a)\right).\end{aligned} \tag{2.37}$$

In numerical calculations, only a finite number of Floquet-Fourier components are retained, and here we will only be concerned with incident electron energies and laser parameters such that threshold effects and laser-induced resonances are negligible. Finally, the differential cross section for the scattering of the electron, having initial energy E_a, into the solid angle $d\Omega$ and emitting k photons, is

$$\frac{d\sigma^k_{ba}}{d\Omega}=\pi^2\frac{p_b}{p_a}\sum_{L,L'=0}^{\infty}[L,L']P_L(\cos\theta)P_{L'}(\cos\theta)[T^k_{p_b,p_a,L}(p_a)]^*T^k_{p_b,p_a,L'}(p_a). \tag{2.38}$$

III. RESULTS AND DISCUSSION

We study laser-assisted electron-He scattering in the static no-exchange approximation. At low energies, it is well known that exchange is important and that the static approximation gives only a fair approximation of the scattering cross section. However, it is not our goal to obtain quantitatively accurate results for laser-assisted scattering of electrons by helium as much as to test the validity of the LFA by treating the model problem exactly. Since for the laser intensities and frequency considered here the polarization of the target by the laser is small [9,12,14], insight into laser-assisted electron-atom scattering in a low-frequency laser field can be gained by investigating, in the first instance, the scattering by the static-direct potential. We note that a LFA for electron-atom scattering has been considered [26] and that a calculation of laser-assisted, low-energy electron-hydrogen in a three-state approximation with exchange has recently been reported [20].

The static potential that we use is obtained from a four-parameter fit to the Hartree-Fock helium ground-state wave function [27] and is given by

$$V_S(r) = -Z\left[\frac{A^2}{4\alpha^3}e^{-2\alpha r}\left(\alpha+\frac{1}{r}\right)+\frac{4AB}{(\alpha+\beta)^3}e^{-(\alpha+\beta)r}\times\left(\frac{(\alpha+\beta)}{2}+\frac{1}{r}\right)+\frac{B^2}{4\beta^3}e^{-2\beta r}\left(\beta+\frac{1}{r}\right)\right]. \quad (3.1)$$

The parameter values are $A=2.605\,05$, $B=2.081\,44$, $\alpha=1.41$, and $\beta=2.61$, and the nuclear charge is $Z=2$. The required potential matrix elements are

$$\langle \mathbf{p}_i|V_S|\mathbf{p}_j\rangle = -\frac{Z}{2\pi^2}\left(\frac{A^2}{4\alpha^3}\frac{2(2\alpha)^2+\Delta_{ij}^2}{[(2\alpha)^2+\Delta_{ij}^2]^2}+\frac{4AB}{(\alpha+\beta)^3}\frac{2(\alpha+\beta)^2+\Delta_{ij}^2}{[(\alpha+\beta)^2+\Delta_{ij}^2]^2}+\frac{B^2}{4\beta^3}\frac{2(2\beta)^2+\Delta_{ij}^2}{[(2\beta)^2+\Delta_{ij}^2]^2}\right). \quad (3.2)$$

The partial-wave expansion of the above potential matrix elements is readily obtained. For example,

$$\frac{2(2\alpha)^2+\Delta_{ij}^2}{[(2\alpha)^2+\Delta_{ij}^2]^2} = \frac{2\pi}{p_i p_j}\sum_{L=0}^{\infty}\sum_{M=-L}^{L} Y_{LM}(\hat{\mathbf{p}}_i)Y_{LM}^*(\hat{\mathbf{p}}_j)\times\left(Q_L(y)+\frac{2\alpha^2}{p_i p_j}\sum_{ll'=0}^{\infty}[l,l']\times\begin{pmatrix} l & l' & L \\ 0 & 0 & 0\end{pmatrix}^2 Q_l(y)Q_{l'}(y)\right), \quad (3.3)$$

with Q_l being a Legendre function of the second kind and $y=[(2\alpha)^2+p_i^2+p_j^2]/(2p_ip_j)$.

Our results have been obtained by numerically solving the half-on-shell partial-wave FLSE. As discussed by Hewitt *et al.* [28], we have used a Gaussian quadrature rule to approximate the integral, with a symmetric interval chosen about the singularity of the kernel. To obtain the functions $\mathcal{J}_{l,l'}^n$, we simply calculate the functions $\mathcal{J}_l^n$ (see Appendix D) on a grid and then use the expression (D4). Typical parameters used in our calculations were, for example, for $\alpha_0=0.4$, 9 partial waves, 17 Floquet-Fourier components, and 36 Gaussian integration points. Higher partial-wave contributions can be readily included, since they are given, to a very good approximation, by their first Born-Volkov amplitudes. While the required matrix elements can be efficiently calculated and the resulting linear system readily inverted, available computer memory is the primary constraint, since as the laser intensity increases, and hence α_0, the number of Floquet-Fourier components and the maximum number of angular momenta required increase rapidly. Our calculations were performed on the Cray J916 at the Brussels Free University Computer Center.

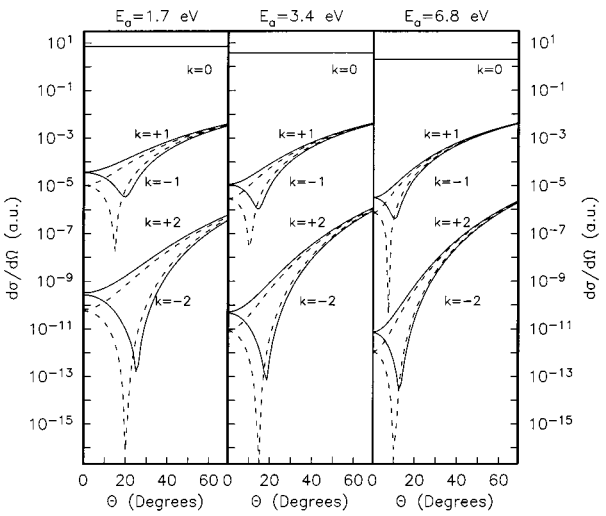

FIG. 1. The laser-assisted partial-differential cross section for scattering of 1.7-, 3.4-, and 6.8-eV electrons by He in the static no-exchange approximation accompanied by the absorption (emission) of $k=0$, ±1, and ±2 photons. The laser frequency is $\omega=0.0043$ a.u. (CO_2 laser) and $\alpha_0=0.2$ a.u., which corresponds to a laser intensity of 4.8×10^5 W/cm^2. The polarization vector of the laser field is parallel to the direction of the incident electron. Shown are the FLSE results (solid lines) and the LFA (dashed lines). Note that for $k=0$ the two results cannot be distinguished here.

We have calculated the laser-assisted differential cross sections for three different incident electron energies and three different laser intensities. The electron energies considered were $E_a=1.7$ eV, $E_a=3.4$ eV, and $E_a=6.8$ eV. For each energy, calculations were made for the laser intensities 4.8×10^5 W/cm^2 (Fig. 1), 1.9×10^6 W/cm^2 (Fig. 2), and 7.7×10^6 W/cm^2 (Fig. 3). The corresponding quiver amplitudes are $\alpha_0=0.2$, $\alpha_0=0.4$, and $\alpha_0=0.8$. The laser frequency was taken to be $\omega=0.0043$ a.u. (CO_2 laser). Our results, as well as the LFA laser-assisted differential cross section, are shown in Figs. 1–3. The solid lines refer to the FLSE results and the broken lines to the zeroth-order Kroll and Watson LFA results [29]. Shown are the elastic cross sections and the cross sections for stimulated emission and absorption of, respectively, one and two photons.

From these figures, we see that, for the laser parameters and incident electron energy considered, the LFA gives,

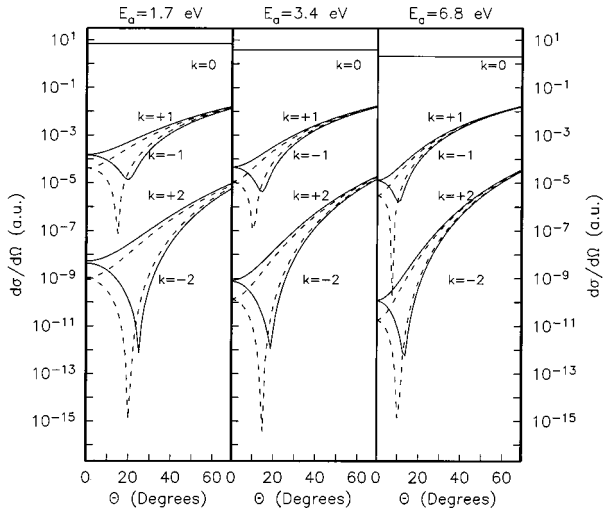

FIG. 2. Same as in Fig. 1; however, $\alpha_0=0.4$, which corresponds to a laser intensity of 1.9×10^6 W/cm^2.

overall, a reasonable approximation of the FLSE differential cross section. There are obviously clear discrepancies in the forward direction. However, the differences are never more than an order of magnitude, with the FLSE cross sections being larger than those of the LFA. For small angles, the positions of the minima in the cross section occur at different angles. In particular, the dips in the cross section given by the LFA are somewhat less pronounced and are slightly shifted to larger angles. We note that the LFA differential cross sections become zero when $\boldsymbol{\Delta}_{ba}\cdot\boldsymbol{\alpha_0}=0$ for $k\neq0$. In the figures, no differences can be discerned between the LFA and FLSE results for elastic scattering ($k=0$). For stimulated absorption (emission) of one or two photons and for scattering angles larger than about 40°, the LFA is a very good approximation. The experimentally observed difference of many orders of magnitude with the Kroll and Watson LFA is not reproduced in our calculations. While the intensities we consider are not as high as the experimental values, our results indicate that the agreement between the FLSE and LFA does not suffer as the laser intensity is increased. The weak-field limit of the FLSE is discussed in Appendix C.

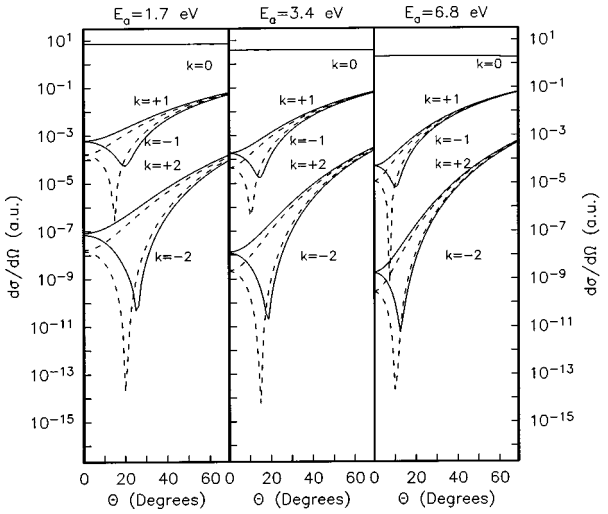

FIG. 3. Same as in Fig. 1; however, $\alpha_0=0.8$, which corresponds to a laser intensity of 7.7×10^6 W/cm^2.

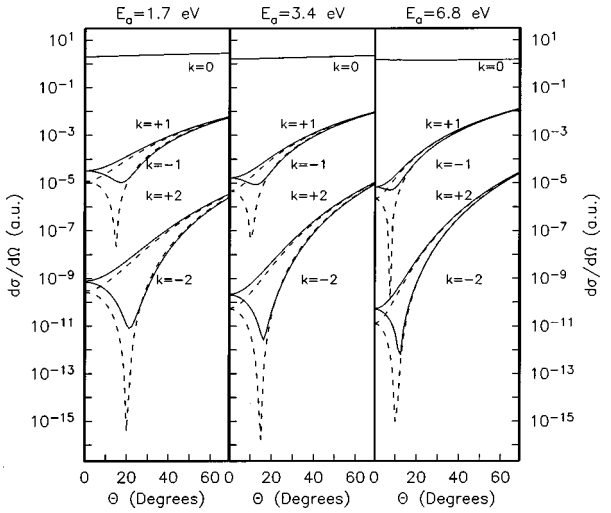

FIG. 4. The laser-assisted partial-differential cross section for scattering of 1.7-, 3.4-, and 6.8-eV electrons by He in the static no-exchange plus polarization (see text) approximation accompanied by the absorption (emission) of $k=0$, ±1, and ±2 photons. The laser frequency is $\omega=0.0043$ a.u. (CO_2 laser) and $\alpha_0=0.4$ a.u. Shown are the FLSE results (solid lines) and the LFA (dashed lines). For $k=0$ the two results cannot be distinguished here.

It is important to stress that the calculated differential cross sections corresponding to photon exchange vary over six or more orders of magnitude, and therefore, due to the sensitive cancellation in the forward direction, nonconvergence in the partial-wave expansion or in the Floquet-Fourier expansion has a dramatic effect on the differential cross section for small scattering angles. Indeed, convergence of the cross sections for backward scattering can be obtained with a minimum Floquet-Fourier expansion, while convergence in the neighborhood of the minimum in the cross section is much more difficult to attain. One way the convergence of the partial wave and Floquet-Fourier expansion can be gauged is by numerically checking the sum rule (A19) in Appendix A.

We have also investigated the effects of a long-range polarization potential by numerically solving the FLSE for scattering by the static direct potential (3.2) plus the Buckingham polarization potential [23]

$$V_p(r)=-\frac{\alpha_p}{2}\frac{1}{(r_c^2+r^2)^2}. \tag{3.4}$$

We have chosen the polarizability $\alpha_p=1.38$ and the cutoff parameter $r_c=1$. The required potential matrix elements are

$$\langle\mathbf{p}_i|V_p|\mathbf{p}_j\rangle=-\frac{\alpha_p}{16\pi r_c}\exp(-\Delta_{ij}r_c). \tag{3.5}$$

In Fig. 4 our results are shown for the same incident electron energies as in the previous figures and for $\alpha_0=0.4$. From this figure it can be seen that the presence of a long-range polarization potential does not affect the accuracy of the LFA, in agreement with previous findings [21,20]. We note that while partial-wave expansions converge very slowly when a long-range polarization potential is present, in our case this did not significantly increase the size of the calculation, since

partial-wave amplitudes for L greater than 9 are very accurately approximated by the correponding first Born-Volkov amplitudes.

IV. CONCLUSIONS

We have described in detail a method for carrying out nonperturbative calculations of laser-assisted electron-potential scattering and we have illustrated the method for electron-helium scattering in a CO_2 laser field in the static no-exchange approximation. Over the range of CO_2 laser intensities and incident electron energies considered, we have found that, overall, the LFA does a reasonable job of predicting the cross sections obtained by solving the FLSE for the geometry in which the incident electron momentum is parallel to the laser polarization direction. While there are clear differences between the FLSE results and the LFA for small angles, both predict a large reduction of the cross sections for small-angle scattering, i.e., when the absorption or emission of photons is classically forbidden [3,22]. Other studies, including classical simulations [8], calculations employing the impulse approximation [17], and nonperturbative calculations [14,21,20,22], have obtained similar results. This is in contrast to the experimental findings [7], in which the measured cross sections near the critical geometries were of the same order of magnitude as away from the critical geometries. Double scattering offers a possible explanation for the experimental results [13,17]. Even a small double-scattering contribution would be sufficient, due to the small cross sections at the critical geometries, to give rise to large enhancements of the cross sections.

Since the Kroll and Watson LFA gives a reasonable approximation to the FLSE results, it is interesting to consider how this approximation can be improved in order to obtain a LFA that is valid at the critical geometries. As is discussed in Appendix B, the zeroth-order Kroll and Watson LFA T-matrix element can be used as the starting point of a low-frequency, iterative scheme that is valid at the critical geometries. The result is the impulse approximation that has been discussed, albeit in a different guise, previously [3,17,18,22]. A comparison of the impulse approximation with exact results for the case of a zero range potential indicates that this approximation is a good one, even at the critical geometries [22].

Finally, we note that experimental and theoretical work has been directed towards testing the robustness of the LFA close to threshold [15,31]. Under these conditions the requirement that the photon energy be small compared with the incident electron energy is not satisfied. The FLSE method discussed here can provide a useful tool for investigating the applicability of the LFA in these cases as well as those involving higher laser frequencies, corresponding to, e.g., the Nd:YAG laser, and the high-frequency limit [30].

ACKNOWLEDGMENTS

This work was supported by the U.K. Engineering and Physical Sciences Research Council (EPSRC), the European Commission ''Human Capital and Mobility'' (HCM) Program, and the Belgian Institut Interuniversitaire des Sciences Nucléaires (IISN). One of us (C.J.J.) would like to thank the Alexander von Humboldt Foundation for finanical support.

APPENDIX A: DERIVATION OF THE KROLL-WATSON LOW-FREQUENCY APPROXIMATION

In this appendix we give a derivation of the Kroll-Watson LFA, starting from the FLSE (2.26). Using Eq. (2.24) we first write Eq. (2.13) as

$$\begin{aligned} T^{(+)k}_{\mathbf{p}_b,\mathbf{p}_a}(E) &= \sum_{l=-\infty}^{\infty} \langle f_{\mathbf{p}_b,k+l}|V|F^{(+)}_{\mathbf{p}_a,m+l}(E)\rangle \\ &= \sum_{l=-\infty}^{\infty} \langle f_{\mathbf{p}_b,k+l}|T^{(+)}(E)|f_{\mathbf{p}_a,m+l}\rangle \\ &= \sum_{l=-\infty}^{\infty} J_{k+l}(\mathbf{p}_b\cdot\boldsymbol{\alpha}_0)J_l(\mathbf{p}_a\cdot\boldsymbol{\alpha}_0)\langle \mathbf{p}_b|T^{(+)}(E)|\mathbf{p}_a\rangle \\ &= J_k(\boldsymbol{\Delta}_{ba}\cdot\boldsymbol{\alpha}_0)\langle \mathbf{p}_b|T^{(+)}(E)|\mathbf{p}_a\rangle, \end{aligned} \tag{A1}$$

so that instead of working with the T-matrix elements evaluated with the ''dressed'' plane waves, we use those evaluated with plane-wave states. With this result, we obtain, after dividing by $J_k(\boldsymbol{\Delta}_{ba}\cdot\boldsymbol{\alpha}_0)$, the following form of the FLSE:

$$\begin{aligned} \langle \mathbf{p}_b|T^{(+)}(E)|\mathbf{p}_a\rangle &= \langle \mathbf{p}_b|V|\mathbf{p}_a\rangle \\ &\quad + \frac{1}{J_k(\boldsymbol{\Delta}_{ba}\cdot\boldsymbol{\alpha}_0)} \sum_{m=-\infty}^{\infty} \int d\mathbf{p}_i \langle \mathbf{p}_b|V|\mathbf{p}_i\rangle \\ &\quad \times \frac{J_{k-m}(\boldsymbol{\Delta}_{bi}\cdot\boldsymbol{\alpha}_0)J_m(\boldsymbol{\Delta}_{ia}\cdot\boldsymbol{\alpha}_0)}{E-(E_i+m\omega)+i\epsilon} \\ &\quad \times \langle \mathbf{p}_i|T^{(+)}(E)|\mathbf{p}_a\rangle. \end{aligned} \tag{A2}$$

Evidently, for $k\neq 0$, if the cross section is to be nonzero when the momentum transfer is perpendicular to the laser polarization, $\langle \mathbf{p}_b|T^{(+)}(E)|\mathbf{p}_a\rangle$ must become arbitrarily large when $\boldsymbol{\Delta}_{ba}\cdot\boldsymbol{\alpha}_0$ goes to zero such that $T^{(+)k}_{\mathbf{k_b}}(E)$ remains finite.

For small frequencies, we expand the energy denominator in the integration kernel in Eq. (A2),

$$\begin{aligned} \frac{1}{E-(E_i+m\omega)+i\epsilon} &= \frac{1}{E-E_i+i\epsilon} \\ &\quad \times \left(1+m\omega\frac{1}{E-E_i+i\epsilon}\right)+\mathcal{O}(\omega^2). \end{aligned} \tag{A3}$$

Now calling $\langle \mathbf{p}_b|T^{(+)(n)}(E)|\mathbf{p}_a\rangle$ the T-matrix element that contains contributions to order ω^n, the zeroth-order approximation can be obtained by setting ω to zero in the denominator of Eq. (A2). Then the summation over m is carried out with the result

$$\langle \mathbf{p}_b|T^{(+)(0)}(E)|\mathbf{p}_a\rangle=\langle \mathbf{p}_b|V|\mathbf{p}_a\rangle+\int d\mathbf{p}_i\langle \mathbf{p}_b|V|\mathbf{p}_i\rangle\frac{1}{E-E_i+\mathrm{i}\epsilon}\langle \mathbf{p}_i|T^{(+)(0)}(E)|\mathbf{p}_a\rangle. \tag{A4}$$

The T-matrix element $\langle \mathbf{p}_b|T^{(+)(0)}(E_a)|\mathbf{p}_a\rangle$ simply satisfies the field-free Lippmann-Schwinger equation.

To first order in ω the low-frequency FLSE is

$$\langle \mathbf{p}_b|T^{(+)(1)}(E)|\mathbf{p}_a\rangle=\langle \mathbf{p}_b|V|\mathbf{p}_a\rangle+\int d\mathbf{p}_i\langle \mathbf{p}_b|V|\mathbf{p}_i\rangle\frac{1}{E-E_i+\mathrm{i}\epsilon}\langle \mathbf{p}_i|T^{(+)(1)}(E)|\mathbf{p}_a\rangle$$
$$+\frac{\omega}{J_k(\boldsymbol{\Delta}_{ba}\cdot\boldsymbol{\alpha}_0)}\sum_{m=-\infty}^{\infty}\int d\mathbf{p}_i\langle \mathbf{p}_b|V|\mathbf{p}_i\rangle\frac{J_{k-m}(\boldsymbol{\Delta}_{bi}\cdot\boldsymbol{\alpha}_0)mJ_m(\boldsymbol{\Delta}_{ia}\cdot\boldsymbol{\alpha}_0)}{(E-E_i+\mathrm{i}\epsilon)^2}\langle \mathbf{p}_i|T^{(+)(1)}(E)|\mathbf{p}_a\rangle. \tag{A5}$$

Carrying out the sum over m gives

$$\langle \mathbf{p}_b|T^{(+)(1)}(E)|\mathbf{p}_a\rangle=\langle \mathbf{p}_b|V|\mathbf{p}_a\rangle+\int d\mathbf{p}_i\langle \mathbf{p}_b|V|\mathbf{p}_i\rangle\left(\frac{1}{E-E_i+\mathrm{i}\epsilon}+\frac{\boldsymbol{\Delta}_{ia}\cdot\boldsymbol{\lambda}}{(E-E_i+\mathrm{i}\epsilon)^2}\right)\langle \mathbf{p}_i|T^{(+)(1)}(E)|\mathbf{p}_a\rangle, \tag{A6}$$

where we have introduced the vector

$$\boldsymbol{\lambda}=\omega\boldsymbol{\alpha}_0\frac{k}{\boldsymbol{\Delta}_{ba}\cdot\boldsymbol{\alpha}_0}. \tag{A7}$$

Keeping terms to order ω, Eq. (A6) is

$$\langle \mathbf{p}_b|T^{(+)(1)}(E)|\mathbf{p}_a\rangle=\langle \mathbf{p}_b|V|\mathbf{p}_a\rangle+\int d\mathbf{p}_i\langle \mathbf{p}_b|V|\mathbf{p}_i\rangle\frac{1}{E-E_i-\boldsymbol{\Delta}_{ia}\cdot\boldsymbol{\lambda}+\mathrm{i}\epsilon}\langle \mathbf{p}_i|T^{(+)(1)}(E)|\mathbf{p}_a\rangle, \tag{A8}$$

so that

$$\langle \mathbf{p}_b|T^{(+)(1)}(E_a)|\mathbf{p}_a\rangle=\langle \mathbf{p}_b|V|\mathbf{p}_a\rangle+2\int d\mathbf{p}_i\langle \mathbf{p}_b|V|\mathbf{p}_i\rangle\frac{1}{|\mathbf{p}_a+\boldsymbol{\lambda}|^2-|\mathbf{p}_i+\boldsymbol{\lambda}|^2+\mathrm{i}\epsilon}\langle \mathbf{p}_i|T^{(+)(1)}(E_a)|\mathbf{p}_a\rangle. \tag{A9}$$

The T-matrix element $\langle \mathbf{p}_b|T^{(1)}(E_a)|\mathbf{p}_a\rangle$ satisfies the same Lippmann-Schwinger equation as the on-shell field-free T-matrix element with the momenta shifted by $\boldsymbol{\lambda}$. Hence, the on-shell T-matrix element is simply

$$\langle \mathbf{p}_b|T^{(1)}(E_a)|\mathbf{p}_a\rangle=\langle \mathbf{p}_b+\boldsymbol{\lambda}|T^{(0)}(\epsilon_a)|\mathbf{p}_a+\boldsymbol{\lambda}\rangle, \tag{A10}$$

with the shifted energy

$$\epsilon_a=E_a+\mathbf{p}_a\cdot\boldsymbol{\lambda}+\frac{1}{2}\lambda^2. \tag{A11}$$

This is the Kroll-Watson LFA, and is valid when $|\boldsymbol{\Delta}_{ba}\cdot\boldsymbol{\alpha}_0|\gg k$ [3,22].

We conclude this appendix by deriving the zeroth-order Kroll-Watson LFA from the partial-wave FLSE (2.34). First the expression (A1) for the T-matrix element is written as

$$T^{(+)k}_{\mathbf{p}_b,\mathbf{p}_a}(E)=\frac{1}{4\pi}\sum_{L=0}^{\infty}[L]P_L(\cos\theta)T^{(+)k}_{p_b,p_a,L}(p)$$
$$=\frac{1}{(4\pi)^3}\sum_{l,l',l''=0}^{\infty}\sum_{L=0}^{\infty}[l,l',l'',L]P_L(\cos\theta)\begin{pmatrix}l & l'' & L\\ 0 & 0 & 0\end{pmatrix}^2\mathcal{J}^k_{l,l'}(p_b\alpha_0,p_a\alpha_0)T^{(+)}_{p_b,p_a,l''}(p), \tag{A12}$$

so that

$$T^{(+)k}_{p_b,p_a,L}(p)=\frac{1}{(4\pi)^2}\sum_{l,l',l''=0}^{\infty}[l,l',l'']\begin{pmatrix}l & l'' & L\\ 0 & 0 & 0\end{pmatrix}^2\mathcal{J}^k_{l,l'}(p_b\alpha_0,p_a\alpha_0)T^{(+)}_{p_b,p_a,l''}(p). \tag{A13}$$

Inserting this expansion for $T^{(+)k}_{p_b,p_a,L}(p)$ into the right-hand side of the partial-wave FLSE (2.34) results in

$$T^{(+)k}_{p_b,p_a,L}(p)=\mathcal{V}^k_L(p_b,p_a,\alpha_0)+2\sum_{m=-\infty}^{\infty}\sum_{L'''=0}^{\infty}[L']\int p_i^2 dp_i \frac{\mathcal{V}^{k,m}_{L,L'}(p_b,p_i,p_a,\alpha_0)}{p^2-(p_i^2+2m\omega)+i\epsilon}T^{(+)}_{p_i,p_a,L'}(p), \tag{A14}$$

with the partial-wave potential matrix elements now being

$$\mathcal{V}^{k,m}_{L,L'}(p_b,p_i,p_a,\alpha_0)$$
$$=\frac{1}{(4\pi)^4}\sum_{l,l',l''=0}^{\infty}\sum_{j,j'=0}^{\infty}[l,l',l'',j,j']\,\Xi_{l',j,l'',L'}\begin{pmatrix} l & l'' & L\\ 0 & 0 & 0\end{pmatrix}^2 V_{l''}(p_b,p_i)\mathcal{J}^{k-m}_{l,l'}(p_b\alpha_0,p_i\alpha_0)\mathcal{J}^{m}_{j,j'}(p_i\alpha_0,p_a\alpha_0), \tag{A15}$$

and we have introduced the symbol

$$\Xi_{l,l',j,j'}=\sum_{L=0}^{\infty}[L]\begin{pmatrix} l & l' & L\\ 0 & 0 & 0\end{pmatrix}^2\begin{pmatrix} j & j' & L\\ 0 & 0 & 0\end{pmatrix}^2. \tag{A16}$$

Before proceeding, we must first calculate a sum involving the functions $\mathcal{J}^n_{l,l'}(a,b)$. A variety of sums can be evaluated using properties of the Bessel functions. For example, the expression

$$J_k(\boldsymbol{\Delta}_{ba}\cdot\boldsymbol{\alpha}_0)=\sum_{m=-\infty}^{\infty}J_{k-m}(\boldsymbol{\Delta}_{bi}\cdot\boldsymbol{\alpha}_0)J_m(\Delta_{ia}\cdot\boldsymbol{\alpha}_0), \tag{A17}$$

together with Eq. (2.33), gives immediately

$$\mathcal{J}^k_{l,l'}(b,a)=\frac{1}{4\pi}\sum_{m=-\infty}^{\infty}\sum_{j=0}^{\infty}[j]\mathcal{J}^{k-m}_{l,j}(b,c)\mathcal{J}^m_{j,l'}(c,a). \tag{A18}$$

An additional sum rule, which we will require, may be derived by again starting with Eq. (A17). Multiplying both sides by, for example, $\langle\mathbf{p}_b|V|\mathbf{p}_i\rangle\langle\mathbf{p}_i|V|\mathbf{p}_a\rangle$, using the partial-wave expansions (2.32) and (2.33), and then integrating over $\hat{\mathbf{p}}_i$, results in

$$\mathcal{J}^k_{l,l'}(b,a)\,\delta_{j'',l''}=\frac{[l'']}{(4\pi)^2}\sum_{m=-\infty}^{\infty}\sum_{jj'=0}^{\infty}[j,j']\,\Xi_{j,l'',j',j''}\,\mathcal{J}^{k-m}_{l,j}(b,c)\mathcal{J}^m_{j',l'}(c,a). \tag{A19}$$

We note that this expression gives a direct method for verifying the numerical convergence of the Floquet and partial-wave expansions used in our calculations. Now retaining the zeroth-order contribution in the expansion for small ω and making use of Eq. (A19), one obtains

$$T^{(+)k(0)}_{p_b,p_a,L}(p)=\frac{1}{(4\pi)^2}\sum_{l,l',l''=0}^{\infty}[l,l,l'']\begin{pmatrix} l & l'' & L\\ 0 & 0 & 0\end{pmatrix}^2\mathcal{J}^k_{l,l'}(p_i\alpha_0,p_j\alpha_0)\left(V_{l''}(p_b,p_a)+2\int p_i^2dp_i\frac{V_{l''}(p_b,p_i)T^{(+)(0)}_{p_i,p_a,l''}(p)}{p^2-p_i^2+i\epsilon}\right). \tag{A20}$$

The superscripts on the T-matrix elements refer, as before, to the fact that we are dealing here with the zeroth-order approximation. Using Eq. (A13), this reduces to

$$T^{(+)(0)}_{p_b,p_a,l''}(p)=V_{l''}(p_b,p_a)+2\int p_i^2dp_i\frac{V_{l''}(p_b,p_i)T^{(+)(0)}_{p_i,p_a,l''}(p)}{p^2-p_i^2+i\epsilon}, \tag{A21}$$

which, as expected, is the partial-wave, field-free scattering Lippmann-Schwinger equation.

APPENDIX B: IMPULSE APPROXIMATION

With the knowledge that, to the zeroth order in the laser frequency, the transition-matrix element $\langle\mathbf{p}_b|T^{(+)(0)}(E_a)|\mathbf{p}_a\rangle$ simply satisfies the field-free Lippmann-Schwinger equation, a simple approximation suggests itself. Using the field-free transition-matrix elements in the right-hand side of Eq. (A2), an improvement to the Kroll and Watson approximation can be obtained that is valid at the critical geometries. As will be demonstrated below, this approximation is just the impulse approximation (IA) that has been discussed in the literature [3,17,18,22].

Our starting point is the IA for the scattering cross section,

$$T^{(+)k(IA)}_{\mathbf{p}_b,\mathbf{p}_a}(E)=\frac{1}{2\pi}\int_0^{2\pi} d\phi \exp(ik\phi-\boldsymbol{\Delta}_{ba}\cdot\boldsymbol{\alpha}_0\sin\phi)\langle \mathbf{p}_b+\mathbf{A}(\phi)/c|T^{(+)(0)}[E_a(\phi)]|\mathbf{p}_a+\mathbf{A}(\phi)/c\rangle, \tag{B1}$$

with $2E_a(\phi)=[\mathbf{p}_a+\mathbf{A}(\phi)/c]^2$. Since the T-matrix element is a solution of the field-free Lippmann-Schwinger equation, Eq. (B1) can be cast in the form

$$T^{(+)k(IA)}_{\mathbf{p}_b,\mathbf{p}_a}(E)=J_k(\boldsymbol{\Delta}_{ba}\cdot\boldsymbol{\alpha}_0)\langle \mathbf{p}_b|V|\mathbf{p}_a\rangle + \frac{1}{2\pi}\int_0^{2\pi} d\phi \exp(ik\phi-\boldsymbol{\Delta}_{ba}\cdot\boldsymbol{\alpha}_0\sin\phi)\int d\mathbf{p}_i \frac{\langle \mathbf{p}_b|V|\mathbf{p}_i\rangle\langle \mathbf{p}_i|T^{(+)(0)}[E_a(\phi)]|\mathbf{p}_a\rangle}{E_a-E_i-\omega\boldsymbol{\Delta}_{ia}\cdot\boldsymbol{\alpha}_0\cos\phi+i\epsilon}. \tag{B2}$$

As in Appendix A, we write to first order in ω,

$$\frac{1}{E_a-E_i-\omega\boldsymbol{\Delta}_{ia}\cdot\boldsymbol{\alpha}_0\cos\phi+i\epsilon}=\frac{1}{E_a-E_i+i\epsilon}\left(1+\frac{\omega\boldsymbol{\Delta}_{ia}\cdot\boldsymbol{\alpha}_0\cos\phi}{E_a-E_i+i\epsilon}\right). \tag{B3}$$

To first order in ω, Eq. (B1) now becomes

$$T^{(+)k(IA)}_{\mathbf{p}_b,\mathbf{p}_a}(E)=J_k(\boldsymbol{\Delta}_{ba}\cdot\boldsymbol{\alpha}_0)\langle \mathbf{p}_b|V|\mathbf{p}_a\rangle+\frac{1}{2\pi}\int_0^{2\pi} d\phi \exp(ik\phi-\boldsymbol{\Delta}_{ba}\cdot\boldsymbol{\alpha}_0\sin\phi) \times\int d\mathbf{p}_i \frac{\langle \mathbf{p}_b|V|\mathbf{p}_i\rangle\langle \mathbf{p}_i|T^{(+)(0)}(E_a)|\mathbf{p}_a\rangle}{E_a-E_i+i\epsilon}\left(1+\frac{\omega\boldsymbol{\Delta}_{ia}\cdot\boldsymbol{\alpha}_0\cos\phi}{E_a-E_i+i\epsilon}\right). \tag{B4}$$

Using the following expansion

$$\left(1+\frac{\omega\boldsymbol{\Delta}_{ia}\cdot\boldsymbol{\alpha}_0\cos\phi}{E_a-E_i+i\epsilon}\right)=\frac{1}{J_k(\boldsymbol{\Delta}_{ba}\cdot\boldsymbol{\alpha}_0)}\sum_{m=-\infty}^{\infty} J_{k-m}(\boldsymbol{\Delta}_{bi}\cdot\boldsymbol{\alpha}_0)J_m(\boldsymbol{\Delta}_{ia}\cdot\boldsymbol{\alpha}_0)\left(1+\frac{m\omega\boldsymbol{\Delta}_{ba}\cdot\boldsymbol{\alpha}_0\cos\phi}{k(E_a-E_i+i\epsilon)}\right), \tag{B5}$$

and performing the integration over ϕ ,

$$\begin{aligned}&\frac{1}{2\pi}\int_0^{2\pi} d\phi \exp(ik\phi-\boldsymbol{\Delta}_{ba}\cdot\boldsymbol{\alpha}_0\sin\phi)\left(1+\frac{m\omega\boldsymbol{\Delta}_{ba}\cdot\boldsymbol{\alpha}_0\cos\phi}{k(E_a-E_i+i\epsilon)}\right)\\ &\quad=J_k(\boldsymbol{\Delta}_{ba}\cdot\boldsymbol{\alpha}_0)+[J_{k+1}(\boldsymbol{\Delta}_{ba}\cdot\boldsymbol{\alpha}_0)+J_{k-1}(\boldsymbol{\Delta}_{ba}\cdot\boldsymbol{\alpha}_0)]\frac{m\omega\boldsymbol{\Delta}_{ba}\cdot\boldsymbol{\alpha}_0}{2k(E_a-E_i+i\epsilon)}\\ &\quad=J_k(\boldsymbol{\Delta}_{ba}\cdot\boldsymbol{\alpha}_0)\left(1+\frac{m\omega}{(E_a-E_i+i\epsilon)}\right),\end{aligned} \tag{B6}$$

gives the final result

$$T^{(+)k(IA)}_{\mathbf{p}_b,\mathbf{p}_a}(E_a)=J_k(\boldsymbol{\Delta}_{ba}\cdot\boldsymbol{\alpha}_0)\langle \mathbf{p}_b|V|\mathbf{p}_a\rangle + \sum_{m=-\infty}^{\infty}\int d\mathbf{p}_i\langle \mathbf{p}_b|V|\mathbf{p}_i\rangle\frac{J_{k-m}(\boldsymbol{\Delta}_{bi}\cdot\boldsymbol{\alpha}_0)J_m(\boldsymbol{\Delta}_{ia}\cdot\boldsymbol{\alpha}_0)}{E_a-(E_i+m\omega)+i\epsilon}\langle \mathbf{p}_i|T^{(+)(0)}(E_a)|\mathbf{p}_a\rangle. \tag{B7}$$

While the evaluation of Eq. (B1) involves only the knowledge of the on-shell T-matrix elements, Eq. (B7) requires that both on-shell and half-on-shell T-matrix elements be known. However, when solving the Lippmann-Schwinger equation for the on-shell T-matrix element, the half-on-shell T-matrix elements are also determined. Moreover, in the form of the IA given by Eq. (B7) the T-matrix elements need be calculated for only one incident energy E_a. These facts would suggest Eq. (B7) as, within the formalism discussed here, a more convenient starting point for calculating the T-matrix elements in the IA.

We now give the expression for the partial-wave T-matrix elements in the IA in terms of the field-free partial-wave T-matrix elements. Expanding these matrix elements as in Eq. (A13) and inserting this into Eq. (A14), gives

$$T^{(+)k(IA)}_{p_b,p_a,L}(p)=\mathcal{V}^k_L(p_b,p_a,\alpha_0)+2\sum_{m=-\infty}^{\infty}\sum_{L'=0}^{\infty}[L'] \times\int p_i^2 dp_i \frac{\mathcal{V}^{k,m}_{L,L'}(p_b,p_i,p_a,\alpha_0)}{p^2-(p_i^2+2m\omega)+i\epsilon}T^{(+)}_{p_i,p_a,L'}(p), \tag{B8}$$

where the partial-wave potential matrix elements $\mathcal{V}^{k,m}_{L,L'}(p_b,p_i,p_a,\alpha_0)$ are defined in Appendix A [see Eq. (A15)].

APPENDIX C: WEAK-FIELD LIMIT

In this appendix, we consider the weak-field limit of the FLSE (2.26). The laser field is parametrized by the quantities ω and $\boldsymbol{\alpha}_0$, and this limit is characterized, for some fixed ω, by $\alpha_0 \ll 0$. Correct to first order in α_0, $T^{(+)0}_{\mathbf{p}_b,\mathbf{p}_a}(E)$ is simply equal to the field-free elastic scattering T-matrix element. The T-matrix elements corresponding to the emission of one photon are of order α_0, and therefore correct to second order in α_0, are given by

$$T^{(+)1}_{\mathbf{p}_b,\mathbf{p}_a}(E)=J_1(\boldsymbol{\Delta}_{ba}\cdot\boldsymbol{\alpha}_0)\langle\mathbf{p}_b|V|\mathbf{p}_a\rangle + \sum_{m=0,1}\int d\mathbf{p}_i J_{1-m}(\boldsymbol{\Delta}_{bi}\cdot\boldsymbol{\alpha}_0) \times\frac{\langle\mathbf{p}_b|V|\mathbf{p}_i\rangle}{E-(E_i+m\omega)+i\epsilon}T^{(+)m}_{\mathbf{p}_i,\mathbf{p}_a}(E). \quad \text{(C1)}$$

A similar expression is obtained for $k=-1$. Continuing in the same manner, the T-matrix elements corresponding to the emission of k photons are of order k in α_0, and hence correct to order $k+1$ in α_0 are

$$T^{(+)k}_{\mathbf{p}_b,\mathbf{p}_a}(E)=V^{k(\mathrm{eff})}_{\mathbf{p}_b,\mathbf{p}_a}(E)+\int d\mathbf{p}_i\frac{\langle\mathbf{p}_b|V|\mathbf{p}_i\rangle}{E-(E_i+k\omega)+i\epsilon}T^{(+)k}_{\mathbf{p}_i,\mathbf{p}_a}(E), \quad \text{(C2)}$$

with

$$V^{k(\mathrm{eff})}_{\mathbf{p}_b,\mathbf{p}_a}(E)=J_k(\boldsymbol{\Delta}_{ba}\cdot\boldsymbol{\alpha}_0)\langle\mathbf{p}_b|V|\mathbf{p}_a\rangle + \sum_{m=0}^{k-1}\int d\mathbf{p}_i J_{k-m}(\boldsymbol{\Delta}_{bi}\cdot\boldsymbol{\alpha}_0) \times\frac{\langle\mathbf{p}_b|V|\mathbf{p}_i\rangle}{E-(E_i+m\omega)+i\epsilon}T^{(+)m}_{\mathbf{p}_i,\mathbf{p}_a}(E). \quad \text{(C3)}$$

These equations provide a recursion relation for the T-matrix elements. Once the on-shell and half-on-shell matrix elements $T^{(+)0}_{\mathbf{p}_b,\mathbf{p}_a}(E)$ have been determined, they are used to calculate an effective inhomogeneous term $V^{k(\mathrm{eff})}_{\mathbf{p}_b,\mathbf{p}_a}(E)$ in a Lippmann-Schwinger-type equation for $T^{(+)1}_{\mathbf{p}_b,\mathbf{p}_a}(E)$. These in turn are used to calculate $T^{(+)2}_{\mathbf{p}_b,\mathbf{p}_a}(E)$, and so forth.

Our results shown in Figs. 1–4 show, at small angles, elastic cross sections that are many orders of magnitude larger than those for absorption and emission. (The difference is much less in the backward direction, with the cross sections for $k\pm1$ being only about an order of magnitude smaller than the elastic cross section.) While this might suggest that a perturbative calculation, as outlined above, could be satisfactory for obtaining the laser-assisted scattering cross sections for the values of α_0 considered here, we would like to emphasize that this is not the case. For example, we could not obtain converged results from a perturbative calculation in which the FLSE was solved with a minimum Floquet-Fourier expansion, i.e., $k=-2,\ldots,2$.

Finally, we note that the zeroth-order LFA, Eq. (A4), can be recovered from the expression (C2), by making use of Eq. (A1) and the fact that, to order $k+1$ in α_0, Eq. (A17) reduces to

$$\sum_{m=0}^{k}J_{k-m}(\boldsymbol{\Delta}_{bi}\cdot\boldsymbol{\alpha}_0)J_m(\boldsymbol{\Delta}_{ia}\cdot\boldsymbol{\alpha}_0)=J_k(\boldsymbol{\Delta}_{ba}\cdot\boldsymbol{\alpha}_0). \quad \text{(C4)}$$

APPENDIX D: SPHERICAL DECOMPOSITION OF THE BESSEL FUNCTIONS

Here we will consider in more detail the functions $\mathcal{J}^k_{l,l'}$ that appear in the partial-wave FLSE (2.34). These functions are defined by

$$\begin{aligned}\mathcal{J}^k_{l,l'}(a,b)&=4\pi^2\int_{-1}^{1}\int_{-1}^{1}dx\,dx'\,J_k(ax-bx')P_l(x)P_l(x')\\&=16\pi i^{-k+l+l'}\int_0^{\pi}d\theta\,j_l(a\cos\theta)j_{l'}(-b\cos\theta)\cos(k\theta)\\&=16\pi i^{-k+l+l'}[1+(-1)^{k+l+l'}]\int_0^{\pi/2}d\theta\,j_l(a\cos\theta)j_{l'}(-b\cos\theta)\cos(k\theta). \quad \text{(D1)}\end{aligned}$$

Clearly $\mathcal{J}^k_{l,l'}$ is zero if $k+l+l'$ is not even.

For computational purposes, it is more convenient to make the following partial-wave expansion of the Bessel function:

$$\begin{aligned}J_k(\boldsymbol{\Delta}_{ij}\cdot\boldsymbol{\alpha}_0)&=\sum_{n=-\infty}^{\infty}J_{k+n}(\mathbf{p}_i\cdot\boldsymbol{\alpha}_0)J_n(\mathbf{p}_j\cdot\boldsymbol{\alpha}_0)\\&=\sum_{n=-\infty}^{\infty}\sum_{l,l'=0}^{\infty}\sum_{m,m'}Y_{lm}(\hat{\mathbf{p}}_i)Y^*_{lm}(\hat{\boldsymbol{\alpha}}_0)Y_{l'm'}(\hat{\mathbf{p}}_j)Y^*_{l'm'}(\hat{\boldsymbol{\alpha}}_0)\mathcal{J}^{k+n}_l(p_i\alpha_0)\mathcal{J}^n_{l'}(p_j\alpha_0), \quad \text{(D2)}\end{aligned}$$

where the functions $\mathcal{J}_l^k$ are defined by

$$\begin{aligned}\mathcal{J}_l^k(a) &= 2\pi \int_{-1}^{1} dx\, J_k(ax) P_l(x) \\ &= 4\mathrm{i}^{l-k} \int_0^{\pi} d\theta\, j_l(a\cos\theta)\cos(k\theta) \\ &= 4\mathrm{i}^{l-k}[1+(-1)^{k+l}] \int_0^{\pi/2} d\theta\, j_l(a\cos\theta)\cos(k\theta),\end{aligned} \tag{D3}$$

and are zero if $l+k \mod 2 \neq 0$. Comparing with Eq. (2.33), $\mathcal{J}_{l,l'}^k$ can be expanded in terms of the functions $\mathcal{J}_l^k$ as

$$\mathcal{J}_{l,l'}^k(a,b) = \sum_{n=-\infty}^{\infty} \mathcal{J}_l^{k+n}(a)\mathcal{J}_{l'}^n(b). \tag{D4}$$

In numerical calculations, therefore, the functions $\mathcal{J}_l^k$ need only be calculated and the required $\mathcal{J}_{l,l'}^n$ are obtained using the relationship (D4).

We now list some of the properties of the functions $\mathcal{J}_l^k$ and $\mathcal{J}_{l,l'}^k$. These follow readily from the properties of the Bessel functions from which they are derived. As with the Bessel functions, we have that

$$\mathcal{J}_l^k(a) = (-1)^k \mathcal{J}_l^{-k}(a). \tag{D5}$$

We also deduce that

$$\begin{aligned}\mathcal{J}_{l,l'}^k(a,b) &= (-1)^{l+l'} \mathcal{J}_{l',l}^k(b,a) = (-1)^k \mathcal{J}_{l,l'}^{-k}(a,b) \\ &= \mathcal{J}_{l',l}^{-k}(b,a).\end{aligned} \tag{D6}$$

Using the well-known series expansion of the Bessel functions, the following series expansions are obtained:

$$\mathcal{J}_l^k(a) = 2\,\mathrm{i}^{l-k}(\pi)^{3/2}\left(\frac{a}{4}\right)^l \sum_{n=0}^{\infty} \frac{(-1)^n \left(\frac{a}{4}\right)^{2n}}{n!\,\Gamma\left(\frac{3}{2}+n+l\right)} \begin{pmatrix} 2n+l \\ \frac{2n+l-|k|}{2} \end{pmatrix}, \tag{D7}$$

$$\mathcal{J}_{l,l'}^k(a,b) = 4\pi^3\,\mathrm{i}^{-k+l+l'}\left(\frac{a}{4}\right)^l\left(-\frac{b}{4}\right)^{l'} \sum_{n,n'=0}^{\infty} \frac{(-1)^{n+n'}\left(\frac{a}{4}\right)^{2n}\left(\frac{b}{4}\right)^{2n'}}{\Gamma\left(l+n+\frac{3}{2}\right)\Gamma\left(l'+n'+\frac{3}{2}\right) n!\,n'!} \begin{pmatrix} 2(n+n')+l+l' \\ \frac{2(n+n')+l+l'-|k|}{2} \end{pmatrix}. \tag{D8}$$

From the recursion relations of the Bessel functions and of the Legendre polynomials, the functions $\mathcal{J}_l^k$ can be shown to satisfy the recursion relations

$$\begin{aligned}\mathcal{J}_l^k(a) &= \frac{a}{2(2l+1)}[\mathcal{J}_{l+1}^{k+1}(a) - \mathcal{J}_{l-1}^{k+1}(a) - \mathcal{J}_{l+1}^{k-1}(a) + \mathcal{J}_{l-1}^{k-1}(a)] \\ &= \frac{a}{2k(2l+1)}\{(l+1)[\mathcal{J}_{l+1}^{k+1}(a) + \mathcal{J}_{l+1}^{k-1}(a)] + l[\mathcal{J}_{l-1}^{k+1}(a) + \mathcal{J}_{l-1}^{k-1}(a)]\}.\end{aligned} \tag{D9}$$

The functions $\mathcal{J}_l^k$ also satisfy

$$\begin{aligned}\frac{d}{da}\mathcal{J}_l^k(a) &= \frac{1}{2}[\mathcal{J}_{l-1}^{k-1}(a) - \mathcal{J}_{l-1}^{k+1}(a)] - \frac{l+1}{a}\mathcal{J}_l^k(a) \\ &= -\frac{1}{2}[\mathcal{J}_{l+1}^{k+1}(a) - \mathcal{J}_{l+1}^{k-1}(a)] + \frac{l}{a}\mathcal{J}_l^k(a) \\ &= \frac{1}{2(2l+1)}\{l[\mathcal{J}_{l-1}^{k-1}(a) - \mathcal{J}_{l-1}^{k+1}(a)] - (l+1)[\mathcal{J}_{l+1}^{k+1}(a) - \mathcal{J}_{l+1}^{k-1}(a)]\} \\ &= \frac{1}{2l+1}[(l+1)\mathcal{J}_{l+1}^{k-1}(a) + l\mathcal{J}_{l-1}^{k-1}(a)] - \frac{k}{a}\mathcal{J}_l^k(a) \\ &= -\frac{1}{2l+1}[(l+1)\mathcal{J}_{l+1}^{k+1}(a) + l\mathcal{J}_{l-1}^{k+1}(a)] + \frac{k}{a}\mathcal{J}_l^k(a),\end{aligned} \tag{D10}$$

and are solutions of the coupled differential equations, for fixed k,

$$\frac{d^2}{da^2}\mathcal{J}_l^k(a)+\frac{1}{a}\frac{d}{da}\mathcal{J}_l^k(a)+\left(\frac{(l+1)^2}{(2l+1)(2l+3)}+\frac{l^2}{(2l+1)(2l-1)}-\frac{k^2}{a^2}\right)\mathcal{J}_l^k(a)$$
$$=-\frac{(l+1)(l+2)}{(2l+1)(2l+3)}\mathcal{J}_{l+2}^k(a)-\frac{l(l-1)}{(2l+1)(2l-1)}\mathcal{J}_{l-2}^k(a), \tag{D11}$$

and for fixed l,

$$\frac{d^2}{da^2}\mathcal{J}_l^k(a)+2\frac{1}{a}\frac{d}{da}\mathcal{J}_l^k(a)+\left(\frac{1}{2}-\frac{l(l+1)}{a^2}\right)\mathcal{J}_l^k(a)=[\mathcal{J}_l^{k+2}(a)+\mathcal{J}_l^{k-2}(a)], \tag{D12}$$

with the boundary conditions

$$\mathcal{J}_l^k(a)\big|_{a=0}=4\pi\,\delta_{k,0}\delta_{l,0},$$
$$\left.\frac{d}{da}\mathcal{J}_l^k(a)\right|_{a=0}=\frac{2}{3}\pi\mathrm{i}^{l-k}\,\delta_{k,\pm l}\delta_{l,1}. \tag{D13}$$

Similar results, though often more complicated, can be obtained for the functions $\mathcal{J}_{l,l'}^k$.

Finally, we consider the partial-wave potential matrix elements (2.35). These functions are zero if $(l+l''+L)\bmod 2\neq 0$, $(l'+l''+L')\bmod 2\neq 0$, or if $(l'+l''+k)\bmod 2\neq 0$. Therefore, they are also zero if $(L+L'+k)\bmod 2\neq 0$, a result that can also be deduced from parity considerations. Indeed, if we define the parity of the T-matrix element $T^{(+)k}_{p_b,p_a,L}(p)$ as $k+L$, the partial-wave potential matrix element $\mathcal{V}^k_{L',L}(p_i\alpha_0,p_j\alpha_0)$ will only couple T-matrix elements of the same parity. This has the important practical consequence that Eq. (2.34) can be solved separately for even- and odd-parity T-matrix elements.

From the properties of $\mathcal{J}_{l,l'}^k$, we also find that

$$\mathcal{V}^k_{L',L}(a,b)=(-1)^{L+L'}\mathcal{V}^k_{L',L}(b,a)$$
$$=(-1)^k\mathcal{V}^{-k}_{L,L'}(a,b)$$
$$=\mathcal{V}^{-k}_{L',L}(b,a). \tag{D14}$$

These relations are also of practical interest when obtaining a numerical solution of Eq. (2.34).

[1] F. Ehlotzky, A. Jaroń, and J. Z. Kamiński, Phys. Rep. **297**, 63 (1998).

[2] F. V. Bunkin and M. V. Fedorov, Zh. Eksp. Teor. Fiz. **49**, 1215 (1966) [Sov. Phys. JETP **22**, 844 (1966)].

[3] N. M. Kroll and K. M. Watson, Phys. Rev. A **8**, 804 (1973).

[4] For example, H. Kruger and C. Jung, Phys. Rev. A **17**, 1706 (1978); M. H. Mittleman, *ibid.* **19**, 134 (1979); **20**, 1965 (1979); L. Rosenberg, Adv. At. Mol. Phys. **18**, 1 (1982); Phys. Rev. A **23**, 2283 (1981); R. Shakeshaft, *ibid.* **28**, 667 (1983); **29**, 383 (1984).

[5] Reviews include F. H. M. Faisal, *Theory of Multiphoton Processes* (Plenum Press, New York, 1987); M. Gavrila, in *Collision Theory for Atoms and Molecules*, edited by F. A. Gianturco (Plenum, New York, 1989), p. 139; P. Francken and C. J. Joachain, J. Opt. Soc. Am. B **7**, 554 (1990); M. H. Mittleman, *Introduction to the Theory of Laser-Atom Interactions* (Plenum Press, New York, 1993); C. J. Joachain, in *Laser Interaction with Atoms, Solids and Plasmas*, edited by R. M. More (Plenum Press, New York, 1994), p. 39.

[6] B. Wallbank, J. K. Holmes, S. C. MacIsaac, and A. Weingartshofer, J. Phys. B **25**, 1265 (1992).

[7] B. Wallbank and J. K. Holmes, Phys. Rev. A **48**, 2515 (1993); J. Phys. B **27**, 1221 (1994); **27**, 5405 (1994).

[8] I. Rabadán, L. Méndez, and A. S. Dickinson, J. Phys. B **27**, L535 (1994).

[9] S. Varró and F. Ehlotzky, Phys. Lett. A **203**, 203 (1995).

[10] S. Varró and F. Ehlotzky, J. Phys. B **28**, L673 (1995); A. S. Dickinson, *ibid.* **29**, 1569 (1996); F. Robicheaux, *ibid.* **29**, 2367 (1996).

[11] L. B. Madsen and K. Taulbjerg, J. Phys. B **28**, 5327 (1995).

[12] S. Geltman, Phys. Rev. A **51**, R34 (1995).

[13] I. Rabadán, L. Méndez, and A. S. Dickinson, J. Phys. B **29**, L801 (1996).

[14] C. T. Chen and F. Robicheaux, J. Phys. B **29**, 345 (1996).

[15] S. Geltman, Phys. Rev. A **53**, 3473 (1996); **55**, 3755 (1997).

[16] A. Cionga, L. Dimou, and F. H. M. Faisal, J. Phys. B **30**, L361 (1997).

[17] D. B. Milosevic and F. Ehlotzky, J. Phys. B **30**, 2999 (1997).

[18] A. Jaroń and J. Z. Kamiński, Phys. Rev. A **56**, R4393 (1997).

[19] I. Rabadán, A. S. Dickinson, and F. Robicheaux, J. Phys. B **31**, 1625 (1998); A. Cionga, L. Dimou, and F. H. M. Faisal, *ibid.* **31**, 1629 (1998).

[20] D. Charlo, M. Terao-Dunseath, K. M. Dunseath, and J.-M. Launay, J. Phys. B **31**, L539 (1998).

[21] N. J. Kylstra and C. J. Joachain, Phys. Rev. A **58**, R26 (1998).

[22] L. B. Madsen and K. Taulbjerg, J. Phys. B **31**, 4701 (1998).

[23] C. J. Joachain, *Quantum Collision Theory* (North-Holland, Amsterdam, 1975).

[24] S-I. Chu, Adv. At. Mol. Phys. **21**, 197 (1985).

[25] E. J. Kelsey and L. Rosenberg, Phys. Rev. A **19**, 756 (1979).

[26] M. H. Mittleman, Phys. Rev. A **21**, 79 (1980); A. Maquet and J. Cooper, *ibid.* **41**, 1724 (1990).

[27] F. W. Byron, Jr. and C. J. Joachain, Phys. Rev. **146**, 1 (1966).

[28] R. N. Hewitt, C. J. Noble, and B. H. Bransden, J. Phys. B **23**, 4185 (1990).

[29] In what follows, the LFA will refer to the zeroth-order Kroll and Watson LFA (see Appendix A).

[30] M. Gavrila and J. Z. Kaminski, Phys. Rev. Lett. **52**, 613 (1984).

[31] B. Wallbank and J. K. Holmes, J. Phys. B **29**, 5881 (1996).